A Dynamical Model for Bark Beetle Outbreaks

Vlastimil Křivan[a,b], Mark Lewis[c], Barbara J. Bentz[d], Sharon Bewick[e], Suzanne M. Lenhart[e], Andrew Liebhold[f]

[a] *Institute of Entomology, Biology Centre, Czech Academy of Sciences, Branišovská 31, 370 05 České Budějovice, Czech Republic*
[b] *Faculty of Sciences, University of South Bohemia, Branišovská 1760, 370 05 České Budějovice, Czech Republic*
[c] *Department of Mathematical and Statistical Sciences, University of Alberta, Edmonton, Canada T6G 2G1*
[d] *USFS Rocky Mountain Research Station, 860 N. 1200 East, Logan, UT 84321*
[e] *National Institute for Mathematical and Biological Synthesis, 1534 White Avenue, Knoxville, TN 37996-1527*
[f] *USDA Forest Service,180 Canfield St., Morgantown, WV 26505 USA*

Abstract

Tree-killing bark beetles are major disturbance agents affecting coniferous forest ecosystems. The role of environmental conditions on driving beetle outbreaks is becoming increasingly important as global climatic change alters environmental factors, such as drought stress, that, in turn, govern tree resistance. Furthermore, dynamics between beetles and trees are highly nonlinear, due to complex aggregation behaviors exhibited by beetles attacking trees. Models have a role to play in helping unravel the effects of variable tree resistance and beetle aggregation on bark beetle outbreaks. In this article we develop a new mathematical model for bark beetle outbreaks using an analogy with epidemiological models. Because the model operates on several distinct time scales, singular perturbation methods are used to simplify the model. The result is a dynamical system that tracks populations of uninfested and infested trees. A limiting case of the model is a discontinuous function of state variables, leading to solutions in the Filippov sense. The model assumes an extensive seed-bank so that tree recruitment is possible even if trees go extinct. Two scenarios are considered for immigration of new beetles. The first is a single tree stand with beetles immigrating from outside while the second considers two forest stands with beetle dispersal between them. For the seed-bank driven recruitment rate, when beetle immigration is low, the forest stand recovers to a beetle-free state. At high beetle immigration rates beetle populations approach an endemic equilibrium state. At intermediate immigration rates, the model predicts bistability as the forest can be in either of the two equilibrium states: a healthy forest, or a forest with an endemic beetle population. The model bistability leads to hysteresis. Interactions between two stands show how a less resistant stand of trees may provide an initial toe-hold for the invasion, which later leads to a regional beetle outbreak in the resistant stand.

Email addresses: vlastimil.krivan@gmail.com (Vlastimil Křivan), mark.lewis@ualberta.ca (Mark Lewis), bbentz@fs.fed.us (Barbara J. Bentz), sharon.bewick@gmail.com (Sharon Bewick), lenhart@math.utk.edu (Suzanne M. Lenhart), aliebhold@fs.fed.us (Andrew Liebhold)

Keywords: bistability, bark beetle, *Dendroctonus ponderosae*, dispersal, Filippov solution, hysteresis, population dynamics, stability, SI models

1. Introduction

Tree-killing bark beetles (Coleoptera: Curculionidae, Scolytinae) are important disturbance agents affecting coniferous forest ecosystems, and population outbreaks have resulted in extensive, landscape scale tree mortality events globally (Schelhaas et al., 2003; Meddens et al., 2012). In their native habitats, bark beetle-caused tree mortality, and its interactions with other disturbances including fire, play key roles in forest succession, species composition, and nutrient cycling (Hicke et al., 2013; Hansen, 2014). Recently, however, changing climate is altering bark beetle outbreak dynamics indirectly, through effects to host trees (Chapman et al., 2012; Gaylord et al., 2013; Hart et al., 2014), and directly, by influencing beetle phenology, voltinism and the probability of survival (Bentz et al., 2010; Safranyik et al., 2010; Bentz et al., 2014; Weed et al., 2015). With continued changes in climate, trajectories of future forest succession will be altered in ways that could have significant negative impacts on other native species as well as on biodiversity in general (Bentz et al., 2010; Fettig et al., 2013).

The biology of tree killing bark beetles is complex and variable. Most species interact in mutualistic relationships with fungi, bacteria, mites and other organisms that provide protection and nutrition, and help in detoxifying host plant chemical defenses (Boone et al., 2013; Hofstetter et al., 2015; Therrien et al., 2015). Native host tree species exhibit formidable constitutive and induced defenses that protect them from bark beetle attacks when beetle population levels are low (Raffa et al., 2008). These defenses, however, can be overcome as beetle numbers increase (Boone et al., 2011). As a result, many tree-killing bark beetle species have evolved chemically-mediated aggregative behaviors that depend on host tree chemicals, and allow them to attack en masse and at higher densities than would be possible in the absence of coordination (Raffa et al., 2008). In contrast, some other bark beetle species lack the feedback mechanisms that facilitate mass attacks and instead colonize host trees that have reduced defenses due to a variety of stressors such as drought, fire or wind injury, and pathogens. The interplay between the threshold dependent colonization success and beetle density, combined with the unique aggregative strategies exhibited by many bark beetle species, leads to complex beetle outbreak dynamics.

The spatial and temporal dynamics of bark beetle population outbreaks will vary across the range of a given species, and also with the level of aggressiveness among species. Population outbreaks of those species without the feedback mechanisms that drive aggregative attacks are rare, and these species exhibit little inter-annual variability in abundance. There are exceptions,

however, including a large drought-driven outbreak of Ips species in the southwestern United States between 2002 and 2004 (Santos and Whitham, 2010). When drought conditions subsided, so did the population outbreak. In contrast, species that exhibit feedback mechanisms facilitating aggregation of large numbers of beetles in order to successfully colonize healthy trees (i.e., aggressive species), including *Dendroctonus ponderosae* and *D. frontalis*, exhibit considerable temporal variability in abundance. Populations can exist at low levels for many years with often rapid eruptions to outbreak levels as a result of population independent processes such as weather or delays, and nonlinearities in density-dependent processes (Berryman, 1982; Martinson et al., 2013). Although the triggers for outbreaks of these aggressive species are varied and not well understood, tree resistance and weather can play large roles. The most resistant trees often also have the greatest food resource for developing beetles but require mass attacks to overwhelm the defenses. Compromised defenses through stressors that include drought (Anderegg et al., 2015) and pathogens (Goheen and Hansen, 1993) can result in a tree being overwhelmed by fewer beetles. This can lead to build up of population in the less resistant trees and eventually becoming large enough to attack more vigorous trees with greater food resources. Indeed, large scale outbreaks of aggressive species require large expanses of relatively vigorous host trees (Fettig et al., 2014). In contrast, species that are incapable of attacking vigorous trees are often found in areas where trees grow on marginal sites and stressed trees are commonly available. For both aggressive and less aggressive beetle species, weather that is favorable for survival and seasonality of beetles and their associates is also required for outbreak initiation (Bentz et al., 2014; Addison et al., 2015; Weed et al., 2015). The complex interaction of tree resistance and weather can result in considerable intra-range variation in population dynamics of a given species as environmental conditions that influence host tree resistance and beetle population dynamics vary temporally and spatially. Low host tree resistance can influence the initiation of outbreaks of aggressive bark beetle species and can sustain outbreaks of less aggressive species.

To better understand the influence of aggressive attacks on trees, we use a susceptible/infective (S/I) model to explore the long-term dynamic interactions between forests ecosystems and bark beetle population dynamics. We assume that tree recruitment is not limited by seeds. We focus our analysis on the effect of tree resistance on the forest state. In particular, we show that, when resistance is low, the forest can be either beetle-free, or can have an endemic beetle population depending on forest history, while, for high resistance, the forest will be beetle-free.

1.1. Review of Existing Models

Several models of bark beetle population dynamics already exist. Here we review and compare the essential features of these models in order to put our current study into context. Given the

importance of temperature in not only triggering but also sustaining bark beetle outbreaks, several models have been developed that incorporate temperature alone (Gilbert et al., 2004; Regniere and Bentz, 2007; Friedenberg et al., 2007) and the combined effects of temperature and host trees (Powell and Bentz, 2009, 2014) on bark beetle population success. For the purpose of this article, however, we restrict ourselves to consideration of simple, strategic models without the effects of climate that are amenable to mathematical analysis of general system properties. To facilitate comparison, we consider similarities and differences in three structural aspects: the representation of forest structure and dynamics, the relationship between beetle density and tree death, and the relationship between tree death and new beetle production.

Because we are interested in the role of host resistance in long-term outbreak dynamics, sensible choices about the representation of natural forest structure and regeneration are essential. Depending on the perspective and scenario under analysis, previous modeling efforts have focused on different aspects of forest structure. Berryman et al. (1984) and Økland and Bjørnstad (2006), for example, modeled a live forest class, and a transient, newly killed tree class that they assumed was not resistant to beetles. Heavilin and Powell (2008) also allowed for two forest classes that differed in their resistance, although, in this study, the less resistant class was allowed at least some level of resistance. More recently, Duncan et al. (2015) developed yet another two-class model. In this case, however, susceptible and resistant classes were mechanistically linked to forest age structure. In reality, of course, stands can be composed of many different types of trees with varying resistance levels. Lewis et al. (2010) accounted for this by allowing any possible distribution of vigor within a stand. Unfortunately, total generality comes at the expense of complicated and analytically intractable models. In the current study, we return to a simpler representation of internally homogeneous forest classes or cohorts consistent with the treatment by Heavilin and Powell (2008) and Duncan et al. (2015).

The crucial mechanism of outbreak initiation is that beetle density exceeds a threshold so that beetles can successfully attack the dominant cohort of trees. One possibility is that resistance of the dominant cohort changes over time. For example, Berryman et al. (1984) assumed that resistance decreases as live stem density increases. In this model, remaining trees regain resistance to attack when an outbreak thinned a stand. Although thinned stands may be less susceptible to attack at low population levels, even thinned stands can be heavily attacked during outbreaks (Fettig et al., 2014). However, in reality, old trees are more susceptible to most tree-killing bark beetles than are young trees, regardless of stand density. An alternative method of varying resistance over time is to explicitly model the transition from highly resistant young trees to more susceptible old trees, as was done in Heavilin and Powell (2008).

Although tree resistance changes dynamically through time due to processes like aging and

crowding, certain forest stands are inherently more or less resistant as a result of environmental factors, e.g., water stress (Anderegg et al., 2015). This spatial aspect of tree resistance has been less well studied from a modeling perspective. Nevertheless, the role of environmental conditions in driving beetle outbreaks will likely become increasingly important as global climatic change alters environmental factors, for example by enlarging regions of drought stress. In this study, rather than focusing on aging and crowding as drivers of outbreak cycles, we instead focus on how spatial and environmental drivers influence host tree resistance and subsequent bark beetle outbreak dynamics.

A final aspect of forest structure and dynamics is regeneration. One approach to modeling forest regeneration (Berryman et al., 1984; Økland and Bjørnstad, 2006) is a standard density-dependent growth model, where growth rate is proportional to the abundance of adult trees, and adult density increases to a carrying capacity. However, pines in particular, are characteristically shade intolerant, and many species such as lodgepole pine, *Pinus contorta*, are characterized by their maintenance of large seed banks of serotinous cones that do not germinate until after a stand replacing disturbance (Johnson and Fryer, 1989). We therefore suggest that a model without recruitment limitation of the tree population may be a better representation of forest dynamics in many of the systems susceptible to aggressive bark beetle outbreaks.

In practice, beetle population density is rarely monitored directly. Instead, the number or proportion of infested trees is used as a proxy for population density (sensu Meddens et al., 2012). To build a simple model that can be compared to data, we follow Heavilin and Powell (2008) and assume that the number of beetles emerging from each successfully attacked tree is independent of the number of beetles that attacked the tree. This assumption is met if the number of beetles required for successful attack is greater than or equal to the number of beetles that can completely exploit tree resources. Other models (Berryman et al., 1984; Powell et al., 1996; Økland and Bjørnstad, 2006; Lewis et al., 2010) have explicitly included intraspecific competition, thereby allowing a more complex relationship between attacking and emerging beetles. Again, however, this detail comes at the expense of model transparency and tractability, thus we prefer the simpler formulation in Heavilin and Powell (2008) and leave more complicated relationships between beetle density and tree infestation for a future study.

When stands are healthy, with a majority of trees that are resistant to beetle attack, it is difficult for low numbers of beetles to overcome tree resistance and colonize stands. Aggressive beetle species, however, are capable of killing trees in resistant stands following a trigger, as described above, and population grows to the outbreak phase (Raffa et al., 2008). Our goal in this paper is to develop a qualitative understanding of how a population outbreak may be facilitated by a three step process. First, there is successful colonization of highly stressed or compromised trees, that have little resistance to bark beetles. Second, there is a build up of beetle densities as beetles exploit

these weakened trees and subsequent spread to surrounding healthy trees. Third, these elevated populations of beetles moving into surrounding healthy trees exceed a threshold and these trees therefore succumb, continuing to feed the expanding epidemic.

Our approach starts by building a detailed mechanistic model for beetle behavior and reproduction and tree dynamics in a single stand. This model is based on simple ideas from epidemiology, extended to include nonlinear resistance thresholds and aggregation (Section 2). To analyze this model, we exploit the very different time scales for beetle behavior and reproduction relative to tree growth. This allows us to use singular perturbation arguments to show how beetle population dynamics exhibit properties such as bistability and hysteresis. Analytical insight of the properties comes from a limiting case that relies on ideas from discontinuous dynamical systems. The three-step colonization process is then understood using a model that describes dynamics in two adjacent stands, one with higher resistance to beetles, and one with lower resistance (Section 3). Using this model, we give analytical conditions that can give rise to a regional outbreak in the resistant stand.

2. One-stand Models

We begin by considering a single stand of trees with uniform resistance. We assume that the trees within this stand can be either bark beetle free, and thus "susceptible", (S), to infestation, or else already colonized by beetles, and thus productively "infected", (I). In what follows we replace "infected" by "infested" which is a more appropriate term in this context. The movement of a tree from the susceptible class to the infested class is then assumed to depend on a sequence of beetle-related events. First, the tree must be found by free-flying beetles, (B), that settle upon its surface, and begin to bore through the bark. Next, these attacking beetles, (A), must effectively survive host tree defenses (e.g., resin) and gain access to the cambium layer. Notably, when the number of beetles per tree is low, individual beetles almost never surmount host defenses, and thus trees only rarely become infested; however as the number of beetles per tree increases, so too does the probability that host tree defenses will be overwhelmed. It is only after beetles have successfully colonized a tree that we consider the tree to be in the infested class. This leads to the following set of four coupled differential equations

$$\begin{aligned} \frac{dS}{dt} &= G(S,I) - \sigma S - \beta(A/S)S \\ \frac{dI}{dt} &= \beta(A/S)S - \sigma I - dI \\ \frac{dB}{dt} &= eI - mB - \lambda BS + \mu \\ \frac{dA}{dt} &= \lambda BS - rA - \beta(A/S)A \end{aligned} \tag{1}$$

where G is a function describing the rate of recruitment of new, susceptible trees within the stand, β is a function describing the rate at which susceptible trees transition into the infested class, λ is

Table 1: State Variables

Symbol	Units	Dimension	Definition
S	trees per hectare	length^{-2}	density of susceptible (beetle free) trees
I	trees per hectare	length^{-2}	density of infested (beetle infested) trees
B	beetles per hectare	length^{-2}	density of free-flying beetles
A	beetles per hectare	length^{-2}	density of attacking beetles
R	beetles per tree	dimensionless	density of attacking beetles per tree

the per beetle per tree rate at which beetles encounter healthy trees, e is the rate at which beetles emerge from an infested tree, σ is the natural mortality rate of healthy trees, d is additional tree mortality that results from beetle infestation, m is the mortality and/or emigration rate of free-flying beetles, r is the mortality rate of attacking beetles and μ describes immigration of beetles from outside the stand. If a tree becomes infested (which occurs at rate β), the number of attacking beetles per tree (A/S) times the density of trees (S) is removed from the beetle pool. This yields the last term in the last equation.

To simplify model analysis, we introduce a change of variables by noting that model (1) can be conveniently expressed using the density of attacking beetles per susceptible tree, $R = A/S$, rather than the absolute density of attacking beetles, A. When this is done, the resulting set of ODEs becomes

$$\begin{aligned} \frac{dS}{dt} &= G(S,I) - \sigma S - \beta(R)S \\ \frac{dI}{dt} &= \beta(R)S - \sigma I - dI \\ \frac{dB}{dt} &= eI - mB - \lambda BS + \mu \\ \frac{dR}{dt} &= \lambda B - R\left(\frac{G(S,I)}{S} + r - \sigma\right). \end{aligned} \tag{2}$$

The state variables are summarized in Table 1.

2.1. Tree recruitment, $G(S, I)$

To model tree recruitment within a conifer stand, we consider the recruitment function $G(S, I) = g(K-S-I)$, where K is the tree carrying capacity of the forest stand and g is a constant describing the rate at which new, susceptible trees become available to beetles. While it might be argued that such a recruitment model is pathological at $S = 0$ (as trees have a positive growth rate), it should be noted that forests can, over a period of years, exhibit recruitment in the absence of seed-producing adults as a result of extensive seed-banks. This is true for conifer forests, since most tree species are characterized by large, long-lived seed banks. As a result, tree recruitment is rarely, if ever, limited by the availability of seed producing adults, although space (e.g., competition for light) is still restrictive.

2.2. Infestation rate, $\beta(R)$

In keeping with threshold-based mortality models, we assume that the rate at which susceptible trees transition into the infested class, $\beta(R)$, exhibits a nonlinear dependence on the number of attacking beetles per susceptible tree (R). This nonlinearity is one of the defining features of bark beetle dynamics, and arises from the fact that most host trees have natural defenses (e.g., resin) that protect against beetle infestation at low beetle densities, but become rapidly overwhelmed at high beetle densities. Accordingly, when beetles are scarce, tree infestation rates are depressed relative to what would be expected on the basis of mass action assumptions. To capture this depression mechanistically we assume a threshold number of attacking beetles per tree (typically dependent on tree resistance), θ, above which infestation succeeds and below which, infestation fails.

We model infestation rate by the Hill function

$$\beta(R) = \beta_0 \frac{R^n}{\Gamma^n + R^n} = \frac{\beta_0}{1 + \Gamma^n R^{-n}} \tag{3}$$

where Γ roughly approximates tree resistance, or the threshold number of beetles required for successful infestation and n is related to the level of beetle aggregation. In particular, low values of n represent high levels of aggregation, while high values of n indicate overdispersion (see Appendix C). To see this, consider the limit $n \to \infty$, wherein $\beta(R)$ defined by (3) becomes a step function. In this limit, an infinitely small increase in beetle density at $R = \Gamma$ leads to a sudden transition from a per tree infestation rate of zero to a per tree infestation rate that is maximal for the system. The abruptness of this transition implies that the addition of an exceedingly small number of new beetles causes every tree to cross the critical infestation threshold simultaneously, which will only happen if beetles are uniform in their distribution over available trees (i.e., in the overdispersion limit).

2.3. Model parameters

Model parameters used in this article are summarized in Table 2. For tree population dynamics, we interpret g as reflecting the rate at which new susceptible adult trees become available to beetles per existing tree at carrying capacity. This parameter is estimated to be approximately 0.05-0.5 years^{-1} for pine trees (Clark et al., 2001). Therefore we set $g = 10^{-4} - 10^{-3}$ day^{-1}. Similarly, because tree species targeted by tree-killing bark beetles can have lifespans between 50 and 500 or more years, depending on the geographic region and beetle species, we set $\sigma = 5 \times 10^{-6} - 5 \times 10^{-5}$ day^{-1}. We assume that beetle infested trees, on the other hand, will produce beetles for approximately 1 year. Thus we set the rate of tree death due to beetle infestation at $d = 3 \times 10^{-3}$ day^{-1}. The length of time before the susceptible tree transfers to the infested class is estimated to range between two weeks and one year and hence β_0 ranges from approximately

$0.003 - 0.07$ day^{-1}. The threshold for succumbing to attack for healthy trees is approximately 10-100 beetles per m^2 of bark area (Lewis et al., 2010). If a tree were between 10 and 20 m tall and had an average diameter between 0.1 and 0.5 m, then its surface area would range between π and $10\pi m^2$. This would mean that the threshold for succumbing to beetle attack would range between 10π and 1000π, i.e., 30-3000 beetles per tree. We assume that tree carrying capacity K is between 100 and 10,000 trees/ha for unmanaged forests (Baker, 2009).

Table 2: Parameter estimates for equation (2) used in this article.

Symbol	Definition	Units	Dimension	Approximate values
g	rate of recruitment of new susceptible trees	per day	time^{-1}	$10^{-4} - 10^{-3}$
σ	death rate of healthy trees	per day	time^{-1}	$(0.5 - 5) \times 10^{-5}$
d	tree death rate due to infestation	per day	time^{-1}	3×10^{-3}
e	per tree rate of beetle emergence	beetles per tree per day	time^{-1}	$10 - 100$
m	death rate of free-flying beetles	per day	time^{-1}	0.05
r	death rate of attacking beetles	per day	time^{-1}	0.1
β_0	maximum rate of infestation of new trees	per day	time^{-1}	$0.003 - 0.07$
λ	rate at which beetles find trees to attack	hectares per tree per day	$\text{length}^2\text{time}^{-1}$	0.001
K	tree carrying capacity	trees per hectare	length^{-2}	$100 - 10,000$
μ	immigration	beetles per hectare per day	$\text{length}^{-2}\text{time}^{-1}$	$0 - 4000$
Γ	beetles per tree necessary for infestation	beetles per tree	dimensionless	$30 - 3000$

Table 3: Non-dimensionalization scheme

Symbol	Approximate Value	Symbol	Approximate Value
$\tilde{S} = \lambda S/m$	state variable	$\tilde{\mu} = \lambda\mu/(em)$	$(0.0002 - 0.002)\mu$
$\tilde{I} = \lambda I/m$	state variable	$\tilde{g} = g/d$	$0.03 - 0.3$
$\tilde{R} = rR/e$	state variable	$\tilde{\beta_0} = \beta_0/d$	$1 - 23$
$\tilde{B} = \lambda B/e$	state variable	$\epsilon_1 = \sigma/d$	$0.002 - 0.016$
$\tilde{t} = dt$	$0.003t$	$\epsilon_2 = d/m$	0.06
$\tilde{K} = \lambda K/m$	$15 - 30$	$\epsilon_3 = d/r$	0.03
$\tilde{\Gamma} = r\Gamma/e$	$0.57 - 15$		

2.4. Non-dimensionalization

We can reduce the number of free parameters through non-dimensionalization. Using the non-dimensionalization schemes outlined in Table 3 gives

$$\begin{aligned} \frac{d\tilde{S}}{d\tilde{t}} &= \tilde{G}(\tilde{S},\tilde{I}) - \epsilon_1\tilde{S} - \frac{\tilde{\beta_0}\tilde{S}\tilde{R}^n}{\tilde{R}^n + \tilde{\Gamma}^n} \\ \frac{d\tilde{I}}{d\tilde{t}} &= \frac{\tilde{\beta_0}\tilde{S}\tilde{R}^n}{\tilde{R}^n + \tilde{\Gamma}^n} - \epsilon_1\tilde{I} - \tilde{I} \\ \epsilon_2\frac{d\tilde{B}}{d\tilde{t}} &= \tilde{I} - \tilde{B} - \tilde{B}\tilde{S} + \tilde{\mu} \\ \epsilon_3\frac{d\tilde{R}}{d\tilde{t}} &= \tilde{B} - \frac{\epsilon_3\tilde{R}\tilde{G}(\tilde{S},\tilde{I})}{\tilde{S}} - \tilde{R} + \epsilon_1\epsilon_3\tilde{R} \end{aligned} \tag{4}$$

where $\tilde{G}(\tilde{S},\tilde{I})$ is the non-dimensionalized recruitment function $\tilde{G}(\tilde{S},\tilde{I}) = \tilde{g}(\tilde{K} - \tilde{S} - \tilde{I})$. Table 3 gives values for dimensionless parameters that correspond to those from Table 2.

2.5. Pseudo-steady state approximation

In general, the dynamics associated with beetle processes, including beetle mortality and tree death due to infestation, are significantly faster than natural tree dynamics. As a result, for realistic parameter values (see, for example, Table 3), it will always be true that $0 < \epsilon_1, \epsilon_2, \epsilon_3 \ll 1$. This allows us to make a pseudo-steady state approximation on (4). Specifically, taking the limit as $\epsilon_1, \epsilon_2, \epsilon_3 \to 0$ we find (in what follows we drop tildes for notational simplicity)

$$\begin{aligned} B &= \frac{I + \mu}{1 + S} \\ R &= B \end{aligned} \tag{5}$$

and

$$\begin{aligned} \frac{dS}{dt} &= G(S,I) - \beta(S,I)S \\ \frac{dI}{dt} &= \beta(S,I)S - I \end{aligned} \tag{6}$$

where

$$\beta(S,I) = \beta_0\frac{(I+\mu)^n}{(I+\mu)^n + \Gamma^n(1+S)^n}. \tag{7}$$

2.6. Scenario one: uniform beetle distribution

We begin our analysis by studying the behavior of the model in the limit that beetles distribute uniformly over available trees (i.e., all trees are equally susceptible and there is no aggregating pheromone). To do this, we take $n \to \infty$ in (7), in which case, the infestation rate, $\beta(S, I)$, becomes a step function. Specifically,

$$\beta(S,I) = \begin{cases} 0 & \text{if } \dfrac{I+\mu}{1+S} < \Gamma \\ \beta_0 & \text{if } \dfrac{I+\mu}{1+S} > \Gamma. \end{cases} \tag{8}$$

From (8) we see that the minimum number of infested trees necessary for beetle spread, I_{min}, can be expressed in terms of the number of susceptible trees, S, according to the expression

$$I_{min}(S) = \Gamma(1+S) - \mu. \tag{9}$$

This threshold is shown by the solid line in Figure 1C, E. It reflects the fact that, if beetles distribute uniformly over available trees, then when there are more susceptible trees, proportionately more beetles are needed to overcome the threshold requirement for infestation. Importantly, when the total number of infested trees falls below the critical threshold for infestation, $I < I_{min}$, model (6) becomes

$$\begin{aligned} \frac{dS}{dt} &= G(S,I) \\ \frac{dI}{dt} &= -I. \end{aligned} \tag{10}$$

The equilibrium solution of (10) is $(S, I) = (K, 0)$. Provided tree resistance is not so small that it can be overcome by beetle immigration from outside, $\mu/(1+K) < \Gamma$, this equilibrium solution satisfies $I < I_{min}(S)$ (Figure 1C, E), it is also the solution to the full system (6), suggesting that long-term dynamics are complete forest recovery and local extinction of beetle population. We remark that when there is no immigration ($\mu = 0$), this is the only possible case. When tree resistance is not sufficient to protect against immigrating beetles, $\Gamma < \mu/(1+K)$, the equilibrium solution of (10) does not fall in the region $I < I_{min}(S)$ (Figure 1A). This is because the solid line from panels C and E shifts to the right of point $(K, 0)$ (and it is thus outside of panel A).

In the part of the phase space where $I > I_{min}(S)$, model (6) becomes

$$\begin{aligned} \frac{dS}{dt} &= G(S,I) - \beta_0 S \\ \frac{dI}{dt} &= \beta_0 S - I. \end{aligned} \tag{11}$$

For $G(S, I) = g(K - S - I)$, (11) has a single endemic equilibrium at

$$(S^*, I^*) = \left(\frac{gK}{g+\beta_0+\beta_0 g}, \frac{gK\beta_0}{g+\beta_0+\beta_0 g} \right). \tag{12}$$

Provided tree resistance is not too high and satisfies

$$\Gamma < \Gamma^* = \frac{gK\beta_0 + \mu(g + \beta_0 + g\beta_0)}{\beta_0 + g + g\beta_0 + gK}, \tag{13}$$

this equilibrium is in the part of the phase space where $I > I_{min}(S)$, and it is locally asymptotically stable there (see Appendix A).

For stressed stands that are subject to a relatively large and constant influx of beetles, i.e., $\Gamma < \mu/(1+K)$, the endemic equilibrium (S^*, I^*) (Figure 1A) is the only locally asymptotically stable equilibrium. However, when tree resistance is intermediate and satisfies $\mu/(1+K) < \Gamma < \Gamma^*$ (we remark that for all parameter values $\mu/(1+K) < \Gamma^*$) there are two locally asymptotically stable equilibria: the beetle free equilibrium $(K, 0)$ and the endemic equilibrium (S^*, I^*) (Figure 1C). Consequently, whether the forest survives or not will depend on its history. Specifically, a fully grown forest with tree densities nearing the forest carrying capacity will be able to resist beetle invasion, whereas a more sparsely populated forest with tree densities well below carrying capacity will not. Notice that this is somewhat counterintuitive, since dense forests provide ample trees for beetles to attack. This, however, is the problem. For uniformly distributing beetles, large numbers of trees dilute the beetle population such that no tree has sufficient beetle loads to become infested. In less dense stands, the dilution effect is not so strong, and there are enough beetles per tree to mount successful attacks. In this system, a large perturbation to the beetle free equilibrium, for example a significant but temporary influx of beetles, can move the system across the line $I = I_{min}(S)$ (solid line in Figure 1C) that divides the two stable states. Ultimately, this means that a one-time influx of beetles can potentially cause the forest to evolve toward the beetle endemic state. For smaller beetle influxes, however, the system will not cross the separatrix, thus once the influx has ceased, the system will return to its initial, beetle-free state. When the tree resistance Γ exceeds Γ^* the beetle free equilibrium $(K, 0)$ is the only asymptotically stable equilibrium and the beetle-free stand will be immune to beetle invasions (Figure 1E). These results are summarized in Table 4. Importantly, intermediate stand resistance that results in bistability leads to a hysteresis loop (Figure 2). When model parameters change slowly, which of the two locally stable equilibria the system finds itself in may depend upon the path taken. For example, Figure 2 considers dependence of the equilibrium infestation on the stand resistance. Let us assume that the stand resistance is high. Then the only equilibrium is the beetle-free forest. As the resistance decreases, the situation will continue to be the same until the lower critical threshold $\mu/(1+K)$ is reached. If the resistance keeps decreasing, there is a sudden jump in the number of infested trees because for low resistance the endemic equilibrium is the only possible state of the forest. Now, let us assume that the resistance starts to increase. The forest will stay in the endemic state until resistance reaches the upper threshold given by Γ^*. For yet higher resistance the beetle-free forest

Table 4: Locally stable equilibria for uniformly dispersing beetles and unlimited tree recruitment

Name	Equilibrium	Resistance	Figure
endemic	$\left(\frac{gK}{g+\beta_0+\beta_0 g}, \frac{gK\beta_0}{g+\beta_0+\beta_0 g}\right)$	$\Gamma < \frac{\mu}{1+K}$	1A
beetle-free/endemic	$(K,0)$, $\left(\frac{gK}{g+\beta_0+\beta_0 g}, \frac{gK\beta_0}{g+\beta_0+\beta_0 g}\right)$	$\frac{\mu}{1+K} < \Gamma < \Gamma^{*\dagger}$	1C
beetle-free	$(K,0)$	$\Gamma^* < \Gamma$	1E

$^\dagger\Gamma^*$ is given by (13)

is the only equilibrium.

Because model (6) with uniform beetle distribution modeled by (8) is a differential equation with a discontinuous right-hand side, solutions are defined in the Filippov sense (Filippov, 1988; Colombo and Křivan, 1993). To ensure existence of solutions, we must analyze what happens along the switching line (9). Appendix B shows that there are two possibilities only. Either trajectories cross the switching line transversally, or trajectories move away from the switching line in both directions (such points are shown e.g., in Figure 1C). In this latter case trajectories of the model are not uniquely defined. Thus, the so called sliding regime does not occur and there are no additional equilibria along the switching line.

2.7. Scenario two: aggregated beetle distribution

To model a nonuniform distribution of beetles over available trees, we take n finite and not too large in (7). Most notably, the basis of attraction for the endemic state at intermediate tree resistance shifts to the right (compare Figure 1C with Figure 1D). The suggestion is that beetles can attack and kill trees in forest stands with higher tree densities when they exhibit aggregative behavior. This, of course, makes intuitive sense. Aggregation counteracts beetle dilution across higher density stands. As a result, the beetle per tree threshold required for infestation is more likely to be met by aggregating beetles, even in stands with large numbers of trees.

3. Two-stand Model

The goal in this section is to derive and analyze a model that gives qualitative understanding of how a regional beetle outbreak may be facilitated by a three step process: (i) infestation of highly stressed or compromised trees, who have little resistance to the beetles; (ii) build up of beetle density in these trees and subsequent spread to surrounding healthy trees; (iii) increase in beetle levels in surrounding healthy trees exceeding a threshold and these trees succumbing to become part of the spreading epidemic.

We consider two forest stands coupled by beetle dispersal. Because we are interested in the role of beetle spillover between stands, we consider forest stands that only differ in terms of resistance,

Γ, and beetle influx from other, more distant sources. Thus model (2) can be extended as follows

$$\begin{aligned}
\frac{dS_1}{dt} &= G_1(S_1, I_1) - \sigma S_1 - \beta_1(R_1) S_1 \\
\frac{dI_1}{dt} &= \beta_1(R_1) S_1 - \sigma I_1 - d I_1 \\
\frac{dB_1}{dt} &= e I_1 - m B_1 - \lambda B_1 S_1 + \delta(B_2 - B_1) + \mu_1 \\
\frac{dR_1}{dt} &= \lambda B_1 - R_1 \left(\frac{G(S_1, I_1)}{S_1} + r - \sigma \right) \\
\frac{dS_2}{dt} &= G_2(S_2, I_2) - \sigma S_2 - \beta_2(R_2) S_2 \\
\frac{dI_2}{dt} &= \beta_2(R_2) S_2 - \sigma I_2 - d I_2 \\
\frac{dB_2}{dt} &= e I_2 - m B_2 - \lambda B_2 S_2 + \delta(B_1 - B_2) + \mu_2 \\
\frac{dR_2}{dt} &= \lambda B_2 - R_2 \left(\frac{G(S_2, I_2)}{S_2} + r - \sigma \right)
\end{aligned} \tag{14}$$

where $\beta_i(R_i) = \beta_0 \frac{R_i^n}{\Gamma_i^n + R_i^n}$, $G_i(S_i, I_i) = g_i(K_i - S_i - I_i)$ and we have assumed that all beetles dispersing from the first stand arrive at the second and vice versa (i.e., they are neither going to nor coming from additional stands) with dispersal rate $\delta > 0$. In addition, there can be stand specific immigration from outside of the two stands (μ_i). Notice that we have not assumed any seed rain between the stands, thus we are considering stands that are geographically distant enough that seed transfer is negligible, however not so distant as to prevent beetles migrating from one stand to the other. Using a direct extension of the non-dimensionalization scheme in Table 3, equation (14) can be rewritten

$$\begin{aligned}
\frac{d\tilde{S}_1}{d\tilde{t}} &= \tilde{G}_1(\tilde{S}_1, \tilde{I}_1) - \epsilon_1 \tilde{S}_1 - \frac{\tilde{\beta}_0 \tilde{S}_1 \tilde{R}_1^n}{\tilde{R}_1^n + \tilde{\Gamma}_1^n} \\
\frac{d\tilde{I}_1}{d\tilde{t}} &= \frac{\tilde{\beta}_0 \tilde{S}_1 \tilde{R}_1^n}{\tilde{R}_1^n + \tilde{\Gamma}_1^n} - \epsilon_1 \tilde{I}_1 - \tilde{I}_1 \\
\epsilon_2 \frac{d\tilde{B}_1}{d\tilde{t}} &= \tilde{I}_1 - \tilde{B}_1 - \tilde{B}_1 \tilde{S}_1 + \tilde{\delta}(\tilde{B}_2 - \tilde{B}_1) + \tilde{\mu}_1 \\
\epsilon_3 \frac{d\tilde{R}_1}{d\tilde{t}} &= \tilde{B}_1 - \epsilon_3 \tilde{R}_1 \frac{\tilde{G}_1(\tilde{S}_1, \tilde{I}_1)}{\tilde{S}_1} - \tilde{R}_1 + \epsilon_1 \epsilon_3 \tilde{R}_1 \\
\frac{d\tilde{S}_2}{d\tilde{t}} &= \tilde{G}_2(\tilde{S}_2, \tilde{I}_2) - \epsilon_1 \tilde{S}_2 - \frac{\tilde{\beta}_0 \tilde{S}_2 \tilde{R}_2^n}{\tilde{R}_2^n + \tilde{\Gamma}_2^n} \\
\frac{d\tilde{I}_2}{d\tilde{t}} &= \frac{\tilde{\beta}_0 \tilde{S}_2 \tilde{R}_2^n}{\tilde{R}_2^n + \tilde{\Gamma}_2^n} - \epsilon_1 \tilde{I}_2 - \tilde{I}_2 \\
\epsilon_2 \frac{d\tilde{B}_2}{d\tilde{t}} &= \tilde{I}_2 - \tilde{B}_2 - \tilde{B}_2 \tilde{S}_2 + \tilde{\delta}(\tilde{B}_1 - \tilde{B}_2) + \tilde{\mu}_2 \\
\epsilon_3 \frac{d\tilde{R}_2}{d\tilde{t}} &= \tilde{B}_2 - \epsilon_3 \tilde{R}_2 \frac{\tilde{G}_2(\tilde{S}_2, \tilde{I}_2)}{\tilde{S}_2} - \tilde{R}_2 + \epsilon_1 \epsilon_3 \tilde{R}_2
\end{aligned} \tag{15}$$

where $\tilde{\delta} = \delta / m$.

Again, taking the limit as $\epsilon_1, \epsilon_2, \epsilon_3 \to 0$ we find the following model under the pseudo-steady state approximation

$$
\begin{aligned}
B_1 &= \frac{I_2\delta + I_1(1+S_2+\delta) + (1+S_2+\delta)\mu_1 + \delta\mu_2}{1+S_2+(2+S_2)\delta + S_1(1+S_2+\delta)} \\
R_1 &= B_1 \\
B_2 &= \frac{I_1\delta + I_2(1+S_1+\delta) + (1+S_1+\delta)\mu_2 + \delta\mu_1}{1+S_2+(2+S_2)\delta + S_1(1+S_2+\delta)} \\
R_2 &= B_2 \\
\frac{dS_1}{dt} &= G_1(S_1,I_1) - \beta_1(S_1,I_1,S_2,I_2)S_1 \\
\frac{dI_1}{dt} &= \beta_1(S_1,I_1,S_2,I_2)S_1 - I_1 \\
\frac{dS_2}{dt} &= G_2(S_2,I_2) - \beta_2(S_2,I_2,S_1,I_1)S_2 \\
\frac{dI_2}{dt} &= \beta_2(S_2,I_2,S_1,I_1)S_2 - I_2
\end{aligned}
\tag{16}
$$

where

$$
\begin{aligned}
\beta_1(S_1,I_1,S_2,I_2) &= \frac{\beta_0}{1+\Gamma_1^n\left(\frac{I_2\delta+I_1(1+S_2+\delta)+(1+S_2+\delta)\mu_1+\delta\mu_2}{1+S_2+(2+S_2)\delta+S_1(1+S_2+\delta)}\right)^{-n}} \\
\beta_2(S_1,I_1,S_2,I_2) &= \frac{\beta_0}{1+\Gamma_2^n\left(\frac{I_1\delta+I_2(1+S_1+\delta)+(1+S_1+\delta)\mu_2+\delta\mu_1}{1+S_2+(2+S_2)\delta+S_1(1+S_2+\delta)}\right)^{-n}}
\end{aligned}
\tag{17}
$$

and tildes have been dropped for notational simplicity.

We analyze the two-stand model by again studying model behavior in the limit that beetles distribute uniformly over available trees ($n \to \infty$ in (17)). As before, this leads to step function infestation rates, $\beta_i(S_i, I_i, S_j, I_j)$, with

$$
\beta_1(S_1,I_1,S_2,I_2) = \begin{cases} 0 & \text{if } \dfrac{I_2\delta + I_1(1+S_2+\delta) + (1+S_2+\delta)\mu_1 + \delta\mu_2}{1+S_2+(2+S_2)\delta + S_1(1+S_2+\delta)} < \Gamma_1 \\ \beta_0 & \text{if } \dfrac{I_2\delta + I_1(1+S_2+\delta) + (1+S_2+\delta)\mu_1 + \delta\mu_2}{1+S_2+(2+S_2)\delta + S_1(1+S_2+\delta)} > \Gamma_1 \end{cases}
\tag{18}
$$

and similarly for β_2. From (18), the minimum number of infested trees necessary for beetle spread in stand 1, $I_{min,1}$, is calculated from equation

$$
\frac{I_2\delta + I_1(1+S_2+\delta) + (1+S_2+\delta)\mu_1 + \delta\mu_2}{1+S_2+(2+S_2)\delta + S_1(1+S_2+\delta)} = \Gamma_1
$$

which yields

$$
I_{min,1}(S_1,S_2,I_2) = \frac{(1+S_1)(1+S_2)\Gamma_1 + (2+S_1+S_2)\Gamma_1\delta - (1+S_2)\mu_1 - \delta(I_2+\mu_1+\mu_2)}{1+S_2+\delta}.
$$

Similar calculations for stand 2 give the critical threshold

$$
I_{min,2}(S_1,S_2,I_1) = \frac{(1+S_1)(1+S_2)\Gamma_2 + (2+S_1+S_2)\Gamma_2\delta - (1+S_1)\mu_2 - \delta(I_1+\mu_1+\mu_2)}{1+S_1+\delta}.
$$

We observe that, due to dispersal, the minimum threshold for infestation to spread in one stand depends on the state of the other stand, i.e., $I_{min,1}$ depends on S_2 and I_2 and, similarly, $I_{min,2}$ depends on S_1 and I_1.

To interpret stand dynamics we consider three possibilities: (a) beetle establishment does not occur in either stand ($I_1 < I_{min,1}$, $I_2 < I_{min,2}$), (b) beetle establishment occurs only in one stand and not in the other (here we assume that establishment occurs in stand 1, i.e., $I_1 > I_{min,1}$, $I_2 < I_{min,2}$), and (c) beetle establishment occurs in both stands ($I_1 > I_{min,1}$, $I_2 > I_{min,2}$).

In the first case, when the beetle population does not reach threshold densities in either stand ($I_1 < I_{min,1}$, $I_2 < I_{min,2}$), model (16) reduces to

$$\begin{aligned} \frac{dS_1}{dt} &= G_1(S_1, I_1) \\ \frac{dI_1}{dt} &= -I_1 \\ \frac{dS_2}{dt} &= G_2(S_2, I_2) \\ \frac{dI_2}{dt} &= -I_2. \end{aligned} \tag{19}$$

The only stable equilibrium of (19) is the beetle-free equilibrium $(S_1^*, I_1^*, S_2^*, I_2^*) = (K_1, 0, K_2, 0)$. This will be a solution to the full system (16) (i.e., belongs to the part of the beetle-free–infested tree phase space where $I_{min,i}(K_1, K_2, 0) > 0 = I_i^*$, $i = 1, 2$) provided tree resistance in both stands is high enough such that $\Gamma_1 > \Gamma_{1a}$ and $\Gamma_2 > \Gamma_{2a}$ (for definition of these and other thresholds below see the footnote of Table 5). We note that, without any immigration from outside (i.e., when $\mu_i = 0$, $i = 1, 2$), the beetle-free state will always exist (as we assume that tree resistance is positive, i.e., $\Gamma_i > 0$, $i = 1, 2$). Sufficient outside immigration to either stand may cause the beetle-free state to disappear in one or both of the stands.

When only the first stand crosses the threshold for infestation ($I_1 > I_{min,1}$, $I_2 < I_{min,2}$), (16) can be written as

$$\begin{aligned} \frac{dS_1}{dt} &= G_1(S_1, I_1) - \beta_0 S_1 \\ \frac{dI_1}{dt} &= \beta_0 S_1 - I_1 \\ \frac{dS_2}{dt} &= G_2(S_2, I_2) \\ \frac{dI_2}{dt} &= -I_2. \end{aligned} \tag{20}$$

Notice that (20) is just a combination of (10) and (11), thus the equilibria of (20), as well as their stability, can be determined directly from the one-stand model. Stand 1 will converge to the endemic equilibrium given by (12) and stand 2 to a beetle-free forest

$$(S_1^*, I_1^*, S_2^*, I_2^*) = \left(\frac{g_1 K_1}{\beta_0 + g_1(1+\beta_0)}, \frac{\beta_0 g_1 K_1}{\beta_0 + g_1(1+\beta_0)}, K_2, 0 \right). \tag{21}$$

The above stand-one endemic/stand-two beetle-free equilibrium will be a solution to the full system (16) (i.e., belongs to the part of the beetle-free–infested tree phase space where $I_1^* > I_{min,1}(S_1^*, S_2^*, I_2^*)$ and $I_2^* = 0 < I_{min,2}(S_1^*, S_2^*, I_1^*)$) provided $\Gamma_1 < \Gamma_{b1}$ and $\Gamma_2 > \Gamma_{b2}$. In other

words, (21) is an equilibrium provided tree resistance in stand 1 is low while tree resistance in stand 2 is high.

Finally, in the case that both stands cross the threshold for establishment ($I_1 > I_{min,1}$, $I_2 > I_{min,2}$), model (16) becomes

$$\begin{aligned} \frac{dS_1}{dt} &= G_1(S_1, I_1) - \beta_0 S_1 \\ \frac{dI_1}{dt} &= \beta_0 S_1 - I_1 \\ \frac{dS_2}{dt} &= G_2(S_2, I_2) - \beta_0 S_2 \\ \frac{dI_2}{dt} &= \beta_0 S_2 - I_2. \end{aligned} \tag{22}$$

Again, the equilibria for (22) as well as their stability can be determined directly from results for the one-stand model. The endemic equilibrium in both stands

$$(S_1^*, I_1^*, S_2^*, I_2^*) = \left(\frac{g_1 K_1}{\beta_0 + g_1(1+\beta_0)}, \frac{\beta_0 g_1 K_1}{\beta_0 + g_1(1+\beta_0)}, \frac{g_2 K_2}{\beta_0 + g_2(1+\beta_0)}, \frac{\beta_0 g_2 K_2}{\beta_0 + g_2(1+\beta_0)} \right). \tag{23}$$

will be a solution to the full system (16) (i.e., belongs to the part of the healthy–infested tree phase space where $I_1^* > I_{min,1}(S_1^*, S_2^*, I_2^*)$ and $I_2^* > I_{min,2}(S_1^*, S_2^*, I_1^*)$) provided $\Gamma_1 < \Gamma_{c1}$ and $\Gamma_2 < \Gamma_{c2}$. In other words, (23) is an equilibrium provided tree resistance in both stands is low. Table 5 summarizes these results.

The effect of beetle dispersal between patches is shown in Figure 3. Here we focus on the following scenario: stand 1 has a lower resistance when compared to stand 2, and there is external immigration of beetles from outside of the system to stand 1 only. Thus, stand 2 can become infested only as a result of beetle dispersal from stand 1, i.e., stand 1 serves as a springboard to infest patch 2. Parameters are such that when immigration to stand 1 is low both stands are in a beetle-free state because resistance is sufficiently high in stand 1 to prevent invasion of beetles. Thus, when immigration is low, we observe a stable equilibrium $(K_1, 0, K_2, 0)$ (Figure 3A,B). As immigration to stand 1 increases, stand 1 shifts to the endemic equilibrium while stand 2 stays beetle-free (Figure 3C,D). For yet higher immigration rates to stand 1 both stands shift to the endemic equilibrium (Figure 3E,F).

Table 5: Two-stand Results for Uniformly Dispersing Beetles

Name	Equilibrium	Tree resistance
beetle-free in both stands	$(K_1, 0, K_2, 0)$	$\Gamma_1 > \Gamma^{\star}_{a1}$, $\Gamma_2 > \Gamma^{\star}_{a2}$
stand 1 endemic, stand 2 beetle-free	$\left(\frac{g_1 K_1}{\beta_0+g_1(1+\beta_0)}, \frac{\beta_0 g_1 K_1}{\beta_0+g_1(1+\beta_0)}, K_2, 0\right)$	$\Gamma_1 < \Gamma^{\dagger}_{b1}$, $\Gamma_2 > \Gamma^{\dagger}_{b2}$
stand 1 beetle-free, stand 2 endemic	$\left(K_1, 0, \frac{g_2 K_2}{\beta_0+g_2(1+\beta_0)}, \frac{\beta_0 g_2 K_2}{\beta_0+g_2(1+\beta_0)}\right)$	$\Gamma_1 > \Gamma_{b1}$, $\Gamma_2 < \Gamma_{b2}$
two-stand endemic	$\left(\frac{g_1 K_1}{\beta_0+g_1(1+\beta_0)}, \frac{\beta_0 g_1 K_1}{\beta_0+g_1(1+\beta_0)}, \frac{g_2 K_2}{\beta_0+g_2(1+\beta_0)}, \frac{\beta_0 g_2 K_2}{\beta_0+g_2(1+\beta_0)}\right)$	$\Gamma_1 < \Gamma^{\ddagger}_{c1}$, $\Gamma_2 < \Gamma^{\ddagger}_{c2}$

421 $^{\star}\Gamma_{a1} = \frac{(1+K_2)\mu_1+\delta(\mu_1+\mu_2)}{1+K_2+(2+K_2)\delta+K_1(1+K_2+\delta)}$, $\Gamma_{a2} = \frac{(1+K_1)\mu_2+\delta(\mu_1+\mu_2)}{1+K_2+(2+K_2)\delta+K_1(1+K_2+\delta)}$

422 $^{\dagger}\Gamma_{b1} = \frac{g_1 K_1\beta_0(1+K_2+\delta)+(g_1+\beta_0+g_1\beta_0)((1+K_2+\delta)\mu_1+\delta\mu_2)}{(1+K_2)(\beta_0+g_1(1+K_1+\beta_0))+(g_1(2+K_1+K_2)+(1+g_1)(2+K_2)\beta_0)\delta}$, $\Gamma_{b2} = \frac{g_1 K_1\beta_0\delta+(g_1+\beta_0+g_1\beta_0)\delta\mu_1+(\beta_0+\beta_0\delta+g_1(1+K_1+\beta_0+\delta+\beta_0\delta))\mu_2}{(1+K_2)(\beta_0+g_1(1+K_1+\beta_0))+(g_1(2+K_1+K_2)+(1+g_1)(2+K_2)\beta_0)\delta}$

423 $^{\ddagger}\Gamma_{c1} = \frac{\left(1+\delta+\frac{g_2 K_2}{g_2+\beta_0+g_2\beta_0}\right)\left(\frac{g_1 K_1\beta_0}{g_1+\beta_0+g_1\beta_0}+\frac{g_2 K_2\beta_0\delta+(g_2+\beta_0+g_2\beta_0)\delta\mu_2}{\beta_0+\beta_0\delta+g_2(1+K_2+\beta_0+\delta+\beta_0\delta)}+\mu_1\right)}{1+2\delta+\frac{g_2 K_2(1+\delta)}{g_2+\beta_0+g_2\beta_0}+\frac{g_1 K_1(\beta_0+\beta_0\delta+g_2(1+K_2+\beta_0+\delta+\beta_0\delta))}{(g_1+\beta_0+g_1\beta_0)(g_2+\beta_0+g_2\beta_0))}}$, $\Gamma_{c2} = \frac{\left(1+\delta+\frac{g_1 K_1}{g_1+\beta_0+g_1\beta_0}\right)\left(\frac{g_2 K_2\beta_0}{g_2+\beta_0+g_2\beta_0}+\frac{g_1 K_1\beta_0\delta+(g_1+\beta_0+g_1\beta_0)\delta\mu_1}{\beta_0+\beta_0\delta+g_1(1+K_1+\beta_0+\delta+\beta_0\delta)}+\mu_2\right)}{1+2\delta+\frac{g_2 K_2(1+\delta)}{g_2+\beta_0+g_2\beta_0}+\frac{g_1 K_1(\beta_0+\beta_0\delta+g_2(1+K_2+\beta_0+\delta+\beta_0\delta))}{(g_1+\beta_0+g_1\beta_0)(g_2+\beta_0+g_2\beta_0))}}$

4. Discussion

4.1. Summary

This paper focuses on the formulation and analysis of a general model for bark beetle outbreaks in continuous time. By capitalizing on the fact that there are multiple time scales involved in the system, we are able to derive a simplified dynamical system that describes the bark beetle population dynamics over long time scales. Further simplifications, using ideas from piecewise dynamics and Filippov dynamical systems (Filippov, 1988; Colombo and Křivan, 1993) allow us to mathematically deduce several key properties of the dynamical model. These include

- Bistability of the forest dynamics arising from a threshold effect with respect to beetle numbers. Here the beetle numbers must exceed a critical value determined by tree resistance to infest healthy trees. Although such threshold effects have been included in previous beetle models, ours is a mechanistically derived threshold, based on tree resistance. Most clearly this is seen in the case of the uniform beetle distribution where the threshold for the invasion splits the forest phase space into two parts, each with its own population dynamics (see the two regions separated by the solid line in Figure 1C). In one region the beetle-free forest is a locally stable equilibrium. In the other part of the phase space an endemic equilibrium is a locally stable equilibrium. The position of these equilibria with respect to the threshold value depends on parameters. However, for parameters that allow coexistence of the beetle-free forest equilibrium and the endemic equilibrium, we get bistability. Depending on the history, the forest can respond to a beetle immigration event either by returning to the beetle-free state, or to move to the endemic state. Bistability carries over also to the case where dispersing beetles show aggregative distribution, modeled by a more gradual Hill function (cf. Figure 1C and D).

- Hysteresis. The model bistability naturally leads to hysteresis effects. These are most easily understood in terms of changes in the stand resistance as illustrated in Figure 2. The lower threshold value for resistance in the hysteresis loop is $\mu/(1+K)$ and the higher value is Γ^* (see eq (13)). These quantities can be directly interpreted in terms of the biological parameters describing the interaction between trees and beetles (Table 2).

- Interactions between multiple patches. Here multiple patches that are spatially linked can interact to produce new outcomes. For example, a less healthy patch of trees may provide a beachhead for the infestation process. Once established, the beetles can then build up in numbers before progressing to neighboring healthy patches of trees, patches that would otherwise be unassailable, and causing them to succumb. These kinds of complex outcomes are illustrated in Figure 3.

- Our model with unlimited tree recruitment rate would be inappropriate for forests that experience complete loss of adult trees over periods longer than the viability of the seed-bank. For this reason we also analyzed the model with the logistic growth (results not showed here). On the contrary to the unlimited recruitment where the forest cannot completely die, the logistic tree recruitment rate has also an extinction equilibrium. In particular, when a forest stand shows a low regeneration rate, as given by the ratio between the rate at which trees become available to beetles relative to the rate at which beetles remove the trees, the stand can go extinct.

4.2. Model Limitations

In model (1) we have made several simplifying assumptions that, though reasonable in many outbreak contexts, will not hold under all scenarios. First, we have taken the rate at which beetles encounter trees, λ, as constant, implying that contact rates between beetles and trees follow a simple mass action law. In reality, however, encounter rates likely exhibit some dependence on both beetle and tree density as well as beetle characteristics, including species-specific search strategies and aggregation behaviors (Mitchell and Preisler, 1991; Safranyik et al., 2010; Powell and Bentz, 2014). Second, we have assumed that the total number of beetles emerging from a tree is independent of the total number of beetles that infested the tree in the first place. More accurately, the rate of emergence should be lower when the number of attacking beetles is far from the carrying capacity of the tree (Light et al., 1983; Anderbrant et al., 1985). Third, we have assumed that the rate at which beetles are killed by host tree defenses, r, is independent of the number of attacking beetles per tree. Realistically, however, the death rate of beetles on trees nearing the threshold for infestation is probably lower than it is on trees with one or a few beetles (Raffa and Berryman, 1983). Furthermore, the threshold, itself, is assumed to be a fixed number, describing the exact number of beetles per tree needed to mount a successful attack. In reality, natural variation between trees would round off this sharp threshold to something more gradual. Fourth, the negative binomial model for beetle attacks necessarily oversimplifies the aggregation process. We are aware that other researchers have developed spatially explicit model with a focus on determining specific attack locations (see, for example, Logan et al., 1998). However, we keep our model spatially implicit by using the negative binomial probability mass function to provide a phenomenological description. This approach has been used before as a baseline probability mass function for the attack density in mountain pine beetle (Chubaty et al., 2009). For generality, we have chosen to model the dynamics in continuous time, although it may be that discrete-time models provide a more accurate description of dynamics, particularly in scenarios where generations are strongly non-overlapping (e.g., species or regions where beetles are univoltine). Additionally, factors such

as environmental stochasticity and interactions with tree signaling chemicals will play a role in the outbreak dynamics.

4.3. Model Extensions

Our modeling approach assumed that each stand comprised a cohort of identical trees. Thus any variation between trees was relegated to the variation found between different stands situated at different locales. In fact, stands are typically composed of several groups of trees, each group with different resistance to infestation and different rate of beetle production. It would be possible to extend the model to include such cases. This would allow us to evaluate the effect of stand structure on beetle outbreak. Some initial attempts in this direction can be found in Lewis et al. (2010), Powell and Bentz (2014) and Duncan et al. (2015). Indeed, it is well known that factors influencing bark beetle infestation are related to stand age and stage. When the characteristics of each group within a stand are determined by age or stage, it is necessary to include stage structure in the underlying dynamical model for the tree population (Koch et al, personal communication). Our analysis that focused on the simplified system where beetles distribute uniformly, leads to general insight that also may apply to the more complex system with clumped beetle populations. For clumped beetle populations the piece-wise linear analysis applied here is not possible and numerical simulations will be necessary to falsify our predictions.

4.4. Concluding Remarks

In summary, our paper has focused on model development and analysis for the dynamics of bark beetle infestation of trees, where tree resistance and beetle aggregation have key roles to play in the infestation outcomes. By carefully formulating a detailed model, and then using perturbation theory to distinguish between the different time scales involved in the infestation process, we are able to derive a remarkably simple system of nonlinear ordinary differential equations for outbreak dynamics. These are further simplified in the limit associated with uniform dispersal of beetles, which gives rise to a Filippov-type dynamical system. Resulting bistable dynamics lead to hysteresis, and the multiple patch dynamics lead to the possibility of less resistant tree populations providing a toe-hold for beetles, from which they build up and eventually outbreak, causing the healthier patch to succumb. By estimating model parameters, based on beetle and tree biology, we are able to show that such behaviors fall within the range of reasonable parameter values.

Acknowledgments

This work was conducted as a part of the Forest Insect Pests Working Group at the National Institute for Mathematical and Biological Synthesis, sponsored by the National Science Foundation, the U.S. Department of Homeland Security, and the U.S. Department of Agriculture through NSF

Award #EF-0832858, with additional support from The University of Tennessee, Knoxville. VK acknowledges support provided by the Institute of Entomology (RVO:60077344). MAL gratefully acknowledges support from NSERC Discovery and Accelerator grants, a Canada Research Chair and a Killam Fellowship. This research was also supported by a grant to MAL from the Natural Science and Engineering Research Council of Canada (grant no. NET GP 434810-12) to the TRIA Network, with contributions from Alberta Agriculture and Forestry, Foothills Research Institute, Manitoba Conservation and Water Stewardship, Natural Resources Canada - Canadian Forest Service, Northwest Territories Environment and Natural Resources, Ontario Ministry of Natural Resources and Forestry, Saskatchewan Ministry of Environment, West Fraser and Weyerhaeuser.

534 Addison, A., Powell, J. A., Bentz, B. J., Six, D. L., 2015. Integrating models to investigate crit-
535 ical phenological overlaps in complex ecological interactions: The mountain pine beetle-fungus
536 symbiosis. Journal of Theoretical Biology 368, 55–66.

537 Anderbrant, O., Schlyter, F., Birgersson, G., 1985. Intraspecific competition affecting parents and
538 offspring in the bark beetle *Ips typographus*. Oikos 45, 89–98.

539 Anderegg, W. R. L., Hicke, J., Fisher, R., Allen, C., Aukema, J., Bentz, B., Hood, S., Lichstein,
540 J., Macalady, A., McDowell, N., Pan, Y., Raffa, K., Sala, A., Shaw, J., Stephenson, N., Tague,
541 C., Zeppel, M., 2015. Tree mortality from drought, insects and their interactions in a changing
542 climate. New Phytologist 208, 674–683.

543 Baker, W. L., 2009. Fire ecology in Rocky Mountain landscapes. Island Press.

544 Bentz, B., Vandygriff, J., Jensen, C., Coleman, T., Maloney, P., Smith, S., Grady, A., Schen-
545 Langenheim, G., 2014. Mountain pine beetle voltinism and life history characteristics across
546 latitudinal and elevational gradients in the western United States. Forest Science 60, 434–449.

547 Bentz, B. J., Régnière, J., Fettig, C. J., Hansen, E. M., Hayes, J. L., Hicke, J. A., Kelsey, R. G.,
548 Negrón, J. F., Seybold, S. J., 2010. Climate change and bark beetles of the western United States
549 and Canada: direct and indirect effects. BioScience 60, 602–613.

550 Berryman, A., Stenseth, N., Wollkind, D., 1984. Metastability of forest ecosystems infested by bark
551 beetles. Researches on Population Ecology 26, 13–29.

552 Berryman, A. A., 1982. Biological-control, thresholds, and pest outbreaks. Environmental Ento-
553 mology 11, 544–549.

554 Boone, C. K., Aukema, B. H., Bohlmann, J., Carroll, A. L., Raffa, K. F., 2011. Efficacy of tree
555 defense physiology varies with bark beetle population density: a basis for positive feedback in
556 eruptive species. Canadian journal of forest research-Revue canadienne de recherche forestiere
557 41, 1174–1188.

558 Boone, C. K., Keefover-Ring, K., Mapes, A. C., Adams, A. S., Bohlmann, J., Raffa, K. F., 2013.
559 Bacteria associated with a tree-killing insect reduce concentrations of plant defense compounds.
560 Journal of Chemical Ecology 39, 1003–1006.

561 Chapman, T. B., Veblen, T. T., Schoennagel, T., 2012. Spatiotemporal patterns of mountain pine
562 beetle activity in the southern Rocky Mountains. Ecology 93, 2175–2185.

563 Chubaty, A. M., Roitberg, B. D., Li, C., 2009. A dynamic host selection model for mountain pine
564 beetle, *Dendroctonus ponderosae* Hopkins. Ecological Modelling 220, 1241–1250.

565 Clark, J. S., Lewis, M., Horvath, L., 2001. Invasion by extremes: population spread with variation
566 in dispersal and reproduction. The American Naturalist 157, 537–554.

567 Colombo, R., Křivan, V., 1993. Selective strategies in food webs. IMA Journal of Mathematics
568 Applied in Medicine and Biology 10, 281–291.

569 Duncan, J. P., Powell, J. A., Gordillo, L. F., Eason, J., 2015. A model for mountain pine beetle
570 outbreaks in an age-structured forest: Predicting severity and outbreak-recovery cycle period.
571 Bull. Math. Biol. 77, 1256–1284.

572 Fettig, C. J., Gibson, K. E., Munson, A. S., Negron, J. F., 2014. Cultural practices for prevention
573 and mitigation of mountain pine beetle infestations. Forest Science 60, 450–463.

574 Fettig, C. J., Reid, M. L., Bentz, B. J., Sevanto, S., Spittlehouse, D. L., Wang, T., 2013. Changing
575 climates, changing forests: A western North American perspective. Journal of Forestry 111, 214–
576 228.

577 Filippov, A. F., 1988. Differential equations with discontinuous righthand sides. Kluwer Academic
578 Publishers, Dordrecht.

579 Friedenberg, N. A., Powell, J. A., Ayres, M. P., 2007. Synchrony's double edge: transient dynamics
580 and the Allee effect in stage structured populations. Ecology Letters 10, 564–573.

581 Gaylord, M. L., Kolb, T. E., Pockman, W. T., Plaut, J. A., Yepez, E. A., Macalady, A. K., Pangle,
582 R. E., McDowell, N. G., 2013. Drought predisposes pinon-juniper woodlands to insect attacks
583 and mortality. New Phytologist 198, 567–578.

584 Gilbert, E., Powell, J., Logan, J., Bentz, B., 2004. Comparison of three models predicting de-
585 velopmental milestones given environmental and individual variation. Bulletin of Mathematical
586 Biology 66, 1821–1850.

587 Goheen, D., Hansen, E., 1993. Effects of pathogens and bark beetles on forests. In: Schowalter, T.,
588 Filip, G. (Eds.), Beetle-pathogen interactions in conifer forests. Academic Press, London, UK,
589 pp. 175–196.

590 Hansen, E. M., 2014. Forest development and carbon dynamics after mountain pine beetle out-
591 breaks. Forest Science 60, 476–488.

592 Hart, S. J., Veblen, T. T., Eisenhart, K. S., Jarvis, D., Kulakowski, D., 2014. Drought induces
593 spruce beetle (*Dendroctonus rufipennis*) outbreaks across northwestern Colorado. Ecology 95,
594 930–939.

595 Heavilin, J., Powell, J., 2008. A novel method for fitting spatio-temporal models to data, with
596 applications to the dynamics of mountain pine beetle. Natural Resource Modelling 21, 489–524.

597 Hicke, J. A., Meddens, A. J. H., Allen, C. D., Kolden, C. A., 2013. Carbon stocks of trees killed
598 by bark beetles and wildfire in the western United States. Environmental Research Letters 8,
599 035032.

600 Hofstetter, R., Dinkins-Bookwalter, J., Davis, T., Klepzig, K., 2015. Symbiotic associations of bark
601 beetles. In: Vega, F. E., Hofstetter, R. W. (Eds.), Bark Beetles: Biology and Ecology of Native
602 and Invasive Species. Academic Press, pp. 209–246.

603 Johnson, E. A., Fryer, G. I., 1989. Population dynamics in lodgepole pine-Engelmann spruce forest.
604 Ecology 70, 1335–1345.

605 Lewis, M. A., Nelson, W., Xu, C., 2010. A structured threshold model for mountain pine beetle
606 outbreak. Bull. Math. Biol. 72, 565–589.

607 Light, D. M., Birch, M. C., Paine, T. D., 1983. Laboratory study of intraspecific and interspecific
608 competition within and between two sympatric bark beetle species, *Ips pini* and *I. paraconfusus*.
609 Zeitschrift für angewandte Entomologie 96, 233–241.

610 Logan, J. A., White, P., Bentz, B. J., Powell, J. A., 1998. Model analysis of spatial patterns in
611 mountain pine beetle outbreaks. Theoretical Population Biology 53, 236–255.

612 Martinson, S. J., Ylioja, T., Sullivan, B. T., Billings, R. F., Ayres, M. P., 2013. Alternate attractors
613 in the population dynamics of a tree-killing bark beetle. Population ecology 55, 95–106.

614 Meddens, A. J. H., Hicke, J. A., Ferguson, C. A., 2012. Spatiotemporal patterns of observed
615 bark beetle-caused tree mortality in British Columbia and the western United States. Ecological
616 Applications 22, 1876–1891.

617 Mitchell, R., Preisler, H., 1991. Analysis of spatial patterns of lodgepole pine attacked by outbreak
618 populations of the mountain pine-beetle. Forest Science 37, 1390–1408.

619 Økland, B., Bjørnstad, O., 2006. A resource-depletion model of forest insect outbreaks. Ecology 87,
620 283–290.

621 Powell, J., Logan, J., Bentz, B., 1996. Local projections for a global model of mountain pine beetle
622 attacks. Journal of theoretical biology 179, 243–260.

623 Powell, J. A., Bentz, B. J., 2009. Connecting phenological predictions with population growth rates
624 for mountain pine beetle, an outbreak insect. Landscape Ecology 24, 657–672.

625 Powell, J. A., Bentz, B. J., 2014. Phenology and density-dependent dispersal predict patterns of
626 mountain pine beetle (*Dendroctonus ponderosae*) impact. Ecological Modelling 273, 173–185.

627 Raffa, K. F., Aukema, B. H., Bentz, B. J., Carroll, A. L., Hicke, J. A., Turner, M. G., Romme,
628 W. H., 2008. Cross-scale drivers of natural disturbances prone to anthropogenic amplification:
629 the dynamics of bark beetle eruptions. Bioscience 58, 501–517.

630 Raffa, K. F., Berryman, A., 1983. The role of host plant-resistance in the colonization behavior and
631 ecology of bark beetles (Coleoptera, Scolytidae). Ecological Monographs 53, 27–49.

632 Regniere, J., Bentz, B., 2007. Modeling cold tolerance in the mountain pine beetle, *Dendroctonus*
633 *ponderosae*. Journal of Insect Physiology 53, 559–572.

634 Safranyik, L., Carroll, A. L., Regniere, J., Langor, D. W., Riel, W. G., Shore, T. L., Peter, B.,
635 Cooke, B. J., Nealis, V. G., Taylor, S. W., 2010. Potential for range expansion of mountain pine
636 beetle into the boreal forest of North America. Canadian entomologist 142, 415–442.

637 Santos, M. J., Whitham, T. G., 2010. Predictors of *Ips confusus* outbreaks during a record drought
638 in southwestern USA: Implications for monitoring and management. Environmental management
639 45, 239–249.

640 Schelhaas, M., Nabuurs, G., Schuck, A., 2003. Natural disturbances in the European forests in the
641 19th and 20th centuries. Global change biology 9, 1620–1633.

642 Therrien, J., Mason, C. J., A., C. J., Adams, A., Aukema, B. H., Currie, C. R., Erbilgin, N., 2015.
643 Bacteria influence mountain pine beetle brood development through interactions with symbiotic
644 and antagonistic fungi: implications for climate-driven host range expansion. Oecologia 179,
645 467–485.

646 Weed, A. S., Bentz, B. J., Ayres, M. P., Holmes, T. P., 2015. Geographically variable response of
647 *Dendroctonus ponderosae* to winter warming in the western United States. Landscape ecology
648 30, 1075–1093.

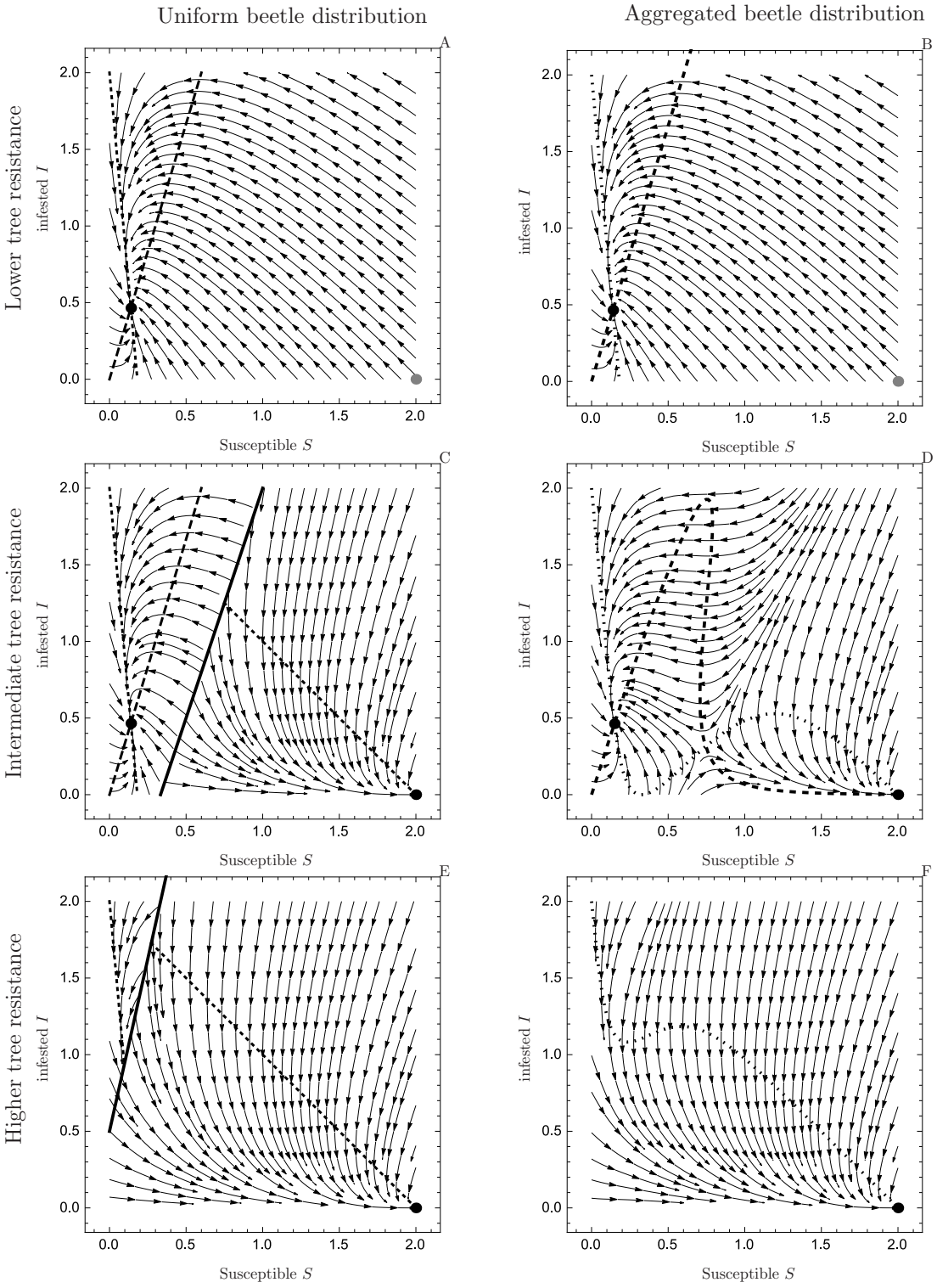

Figure 1: These plots show trajectories of model (6) for uniform beetle distribution (β is given by (8)) (left panels) and aggregated beetle distribution (β is given by (7) with $n = 10$) (right panels). Panels A and B assume low tree resistance ($\Gamma = 30$), panels C and D assume intermediate resistance ($\Gamma = 300$), and panels E and F assume high resistance ($\Gamma = 450$). The solid line in panels C and E is the threshold I_{min} for infestation given by (9) above which beetle spread in the forest. The dotted line is the isocline for susceptible trees and the dashed line is the isocline for infested trees. The black dot denotes a locally stable equilibrium, while the gray dot denotes an unstable equilibrium. Other untransformed parameters are: $g = 0.001$, $d = 0.003$, $m = 0.05$, $\beta_0 = 0.01$, $\mu = 2000$, $K = 100$. For simulations these parameters were non-dimensionalized following scheme in Table 3.

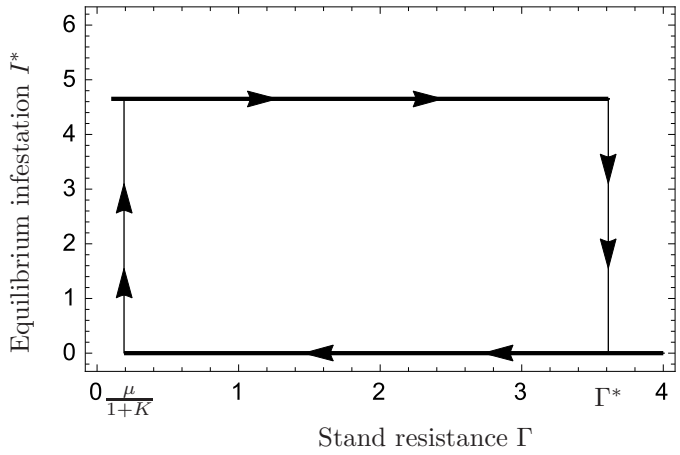

Figure 2: Dependence of the equilibrium infestation I^* on the transformed stand resistance. This figure documents hysteresis in the forest dynamics. Untransformed parameters: $g = 0.001$, $d = 0.003$, $m = 0.05$, $\beta_0 = 0.01$, $\mu = 2000$, $K = 1000$. For simulations these parameters were non-dimensionalized following scheme in Table 3

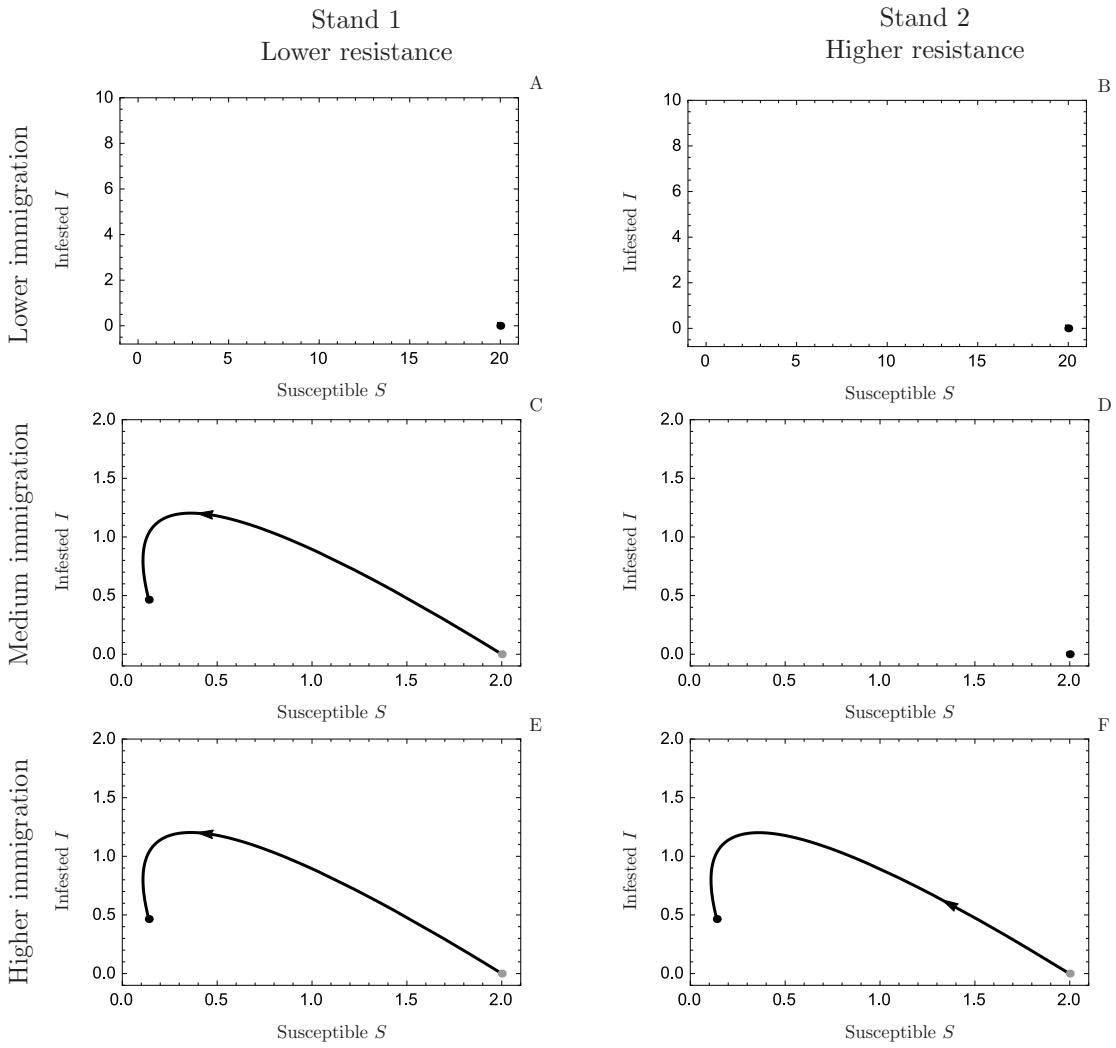

Figure 3: The springboard effect of stand 1 on the beetle outbreak in stand 2. These plots assume that beetles disperse between two forest stands and there is an allochthonous beetle inflow to stand 1 (but not to stand 2). Stand 1 has a lower resistance ($\Gamma_1 = 30$) when compared to stand 2 ($\Gamma_2 = 200$). When immigration of beetles to stand 1 from outside of the system is relatively small (panels A, B; $\mu_1 = 100$, $\mu_2 = 0$), both stands stay at the beetle-free state. For intermediate immigration rates to stand 1 (panels C, D; $\mu_1 = 1000$, $\mu_2 = 0$), stand 1 shifts to the endemic equilibrium (12) while stand 2 stays at the beetle-free state. For high immigration rates to stand 1 (panels E, F; $\mu_1 = 4000$, $\mu_2 = 0$), both stands shift to the endemic equilibrium. Besides the above differences, both stands are assumed to be identical. The curve is a trajectory of model (16) when beetles distribute uniformly over available trees. The black dot denotes a locally stable equilibrium, while the gray dot denotes an unstable equilibrium. Untransformed parameters used for simulations: $\beta_0 = 0.01$ $\lambda_1 = \lambda_2 = 0.001$, $g_1 = g_2 = 0.001$, $r_1 = r_2 = 0.1$, $m_1 = m_2 = 0.05$, $d_1 = d_2 = 0.003$, $K_1 = K_2 = 100$, $\delta = 10$, $e = 10$. For simulations these parameters were non-dimensionalized following scheme in Table 3.

Appendix A. Local stability analysis

Model (11) defines a linear system with matrix

$$A = \begin{pmatrix} -g-\beta_0 & -g \\ \beta_0 & -1 \end{pmatrix}. \tag{A.1}$$

Because the trace of A is given by $Tr(A) = -1-g-\beta_0$, while the determinant of A is given by $Det(A) = g+\beta_0+g\beta_0$, both eigenvalues of A have negative real parts for positive parameter values. Accordingly, the endemic equilibrium (12) will be asymptotically stable.

Appendix B. Behavior of trajectories of model (6) and (8) along the discontinuity line

We study behavior of trajectories along the switching line $I = \Gamma(1+S)-\mu$. The gradient vector to this line is $n = \{-\Gamma, 1\}$. Let f_1 denote the right hand side of (10) and f_2 denote the right hand side of (11), respectivelly. Then

$$\langle n, f_2\rangle = \langle n, f_1\rangle + S\beta_0(1+\Gamma),$$

where $\langle ., .\rangle$ denotes the scalar product. It follows that if $\langle n, f_1\rangle > 0$ then $\langle n, f_2\rangle > 0$, or, similarly, if $\langle n, f_2\rangle < 0$ then $\langle n, f_1\rangle < 0$. These are the conditions that exclude the possibility where $\langle n, f_1\rangle > 0$ and $\langle n, f_2\rangle < 0$. In other words, trajectories of model (6) are never pushed both from above and from below to the switching line. This also shows that no "sliding regime" sensu Filippov (1988) (see also Colombo and Křivan, 1993) occurs. Additionally, no locally stable equilibria can exist at the switching line.

Appendix C. Relation between beetle aggregation and steepness of the Hill function

We assume that a critical number of beetles, θ, are needed to overcome tree defenses. Therefore the probability that any given tree is overcome by the beetles can be determined by evaluating the probability that the random variable X, that describes the number of beetles per tree, is greater than θ. When $X > \theta$, tree infestation occurs at rate β_0, and no trees become infested when $X \leq \theta$. Defining, $F(x, R) = \Pr\{X \leq x \mid \bar{X} = R\}$ as the lower tail of the cumulative distribution function F with the mean of the random variable X equal to $\bar{X}$, we observe that $\Pr\{X > \theta \mid \bar{X} = R\} = 1 - F(\theta, R)$. Our assumption that trees are infested at rate β_0 when $X > \theta$, and that no trees become infested when $X \leq \theta$ gives the rate of infestation of new trees, $\beta(R)$, in terms of $F(\theta, R)$ as

$$\beta(R) = \beta_0(1 - F(\theta, R)). \tag{C.1}$$

Beetle random dispersal is often described by a Poisson distribution $Pois(R)$. We do not include the specifics of active aggregation with respect to pheromones in the analysis. An approach

pioneered for insects by Waters (1959) and popularized by May (1978), subsumes the spatial and behavioral complexities that lead to patterns of aggregation into the single phenomenological assumption that the net distribution of attacks upon hosts is of negative binomial form. Although this was initially developed for parasitoids rather than bark beetles, the underlying modeling philosophy is the same. In this case the Negative Binomial distribution has mean $\bar{X} = R$ and dispersion parameter k, and is denoted by $NB(R, k)$. Unfortunately, because $F(\theta, R)$ is a complex cumulative distribution function, it creates difficulties in terms of model analysis. We therefore replace $F(\theta, R)$ in (C.1) with a Hill function capable of caricaturing the cumulative distribution function (Figure Appendix C.1). We do not claim that the Hill function is a perfect approximation for the cumulative distribution function for the negative binomial, only that it is an appropriate caricature for the degree of precision needed for the modeling at hand. Parameter Γ in the Hill function (3) approximates the threshold number of beetles required for successful infestation, θ, while n plays a role similar to the dispersion parameter, k. In particular, low values of n represent high levels of aggregation, while high values of n indicate overdispersion (see Figure Appendix C.1). If, for example, we assume that successful colonization of moderate size trees requires $\theta = 1000$ beetles per tree, then by comparing the Hill function in equation (3) to the expression that it approximates in equation (C.1) and assuming either the Negative Binomial or Poisson distribution for $F(\theta, R)$, we can find the value of n and Γ that best approximates the beetle distribution. The right panel of Figure 1 shows the case when $n = 10$. Note that the qualitative behavior is similar to that of the uniform beetle scenario although the quantitative details differ.

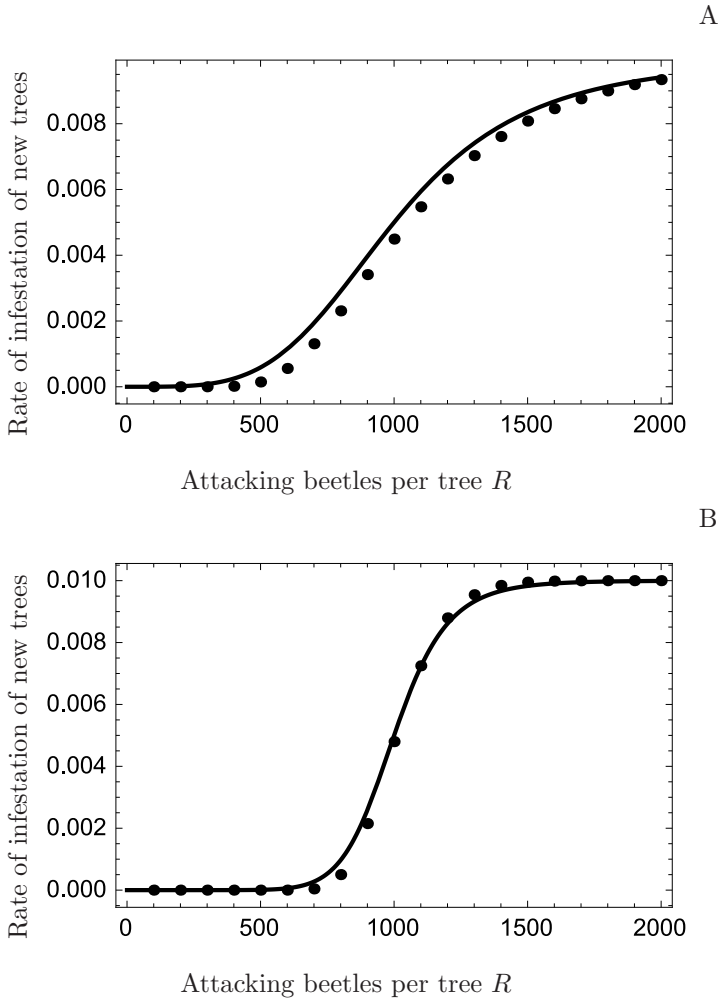

Figure Appendix C.1: Comparison of the rate of infestation of new trees (C.1) (dots) and its approximation by the Hill model (3) (line). Model (C.1) assumes a Negative Binomial distribution with $\theta = 1000$ and dispersion parameter $k = 7$ in panel A and $k = 50$ in panel B. Model (3) assumes $\Gamma = 1000$ and $n = 4$ in panel A and $n = 10$ in panel B. In both panels $\beta_0 = 0.01$.